3rd URSI AT-AP-RASC, Gran Canaria, 29 May – 3 June 2022

A Fast RFI Mitigation Approach via Alternating Projection in Real SAR Data

Yan Huang*(1), Ruizhe Zhang(1), Jiang Liu(1), Zhangcheng Hao(1), Guisheng Liao(2), and Wei Hong(1)
(1) State Key Lab of Millimeter Waves, School of Information Science and Engineering, Southeast University, Nanjing, China
(2) National Key Lab of Radar Signal Processing, Xidian University, Xi'an, China

Abstract

As a wideband radar system, the synthetic aperture radar (SAR) system may conflict with several electromagnetic systems, such as frequency modulation (FM), TV, and other communication systems. These signals, called radio frequency interference (RFI) for radar systems, severely interfere SAR systems from generating a high-resolution image. Many previous researches focused on the RFI suppression problem, among which the semi-parametric methods have been verified to realize the state-of-the-art (SOTA) performance. However, most of the semi-parametric methods are computationally expensive and can hardly be used on the wide-swath SAR imaging processing. Hence in this paper, an efficient semi-parametric algorithm is proposed to suppress RFIs via alternating projections. It has comparable performance as the other SOTA methods and improves the computational efficiency a lot. The real SAR data is provided to demonstrate the effectiveness and efficiency of the proposed algorithm.

1 Introduction

Synthetic aperture radar (SAR) has attracted world-wide attention due to its ability to generate high-resolution wide-swath (HRWS) SAR images under all weather and daylight conditions[1, 2]. As the wideband radar system, SAR systems are often interfered by other electromagnetic systems, such as communication systems, frequency modulation (FM), and TV systems, which are classified as the radio-frequency interference (RFI) [3]. For an RFI, its bandwidth is commonly much less than that of SAR transmitted signals and regarded as a special kind of narrowband interferences (NBIs) (ref. [4] defines the bandwidth ratio to 1%). In practice, SAR systems have potential interference suppression ability via its two-dimensional (2-D) accumulation. Nevertheless, the power of RFI is usually much stronger than the real echoes, which results in quite low signal-to-interference-and-noise ratio (SINR) and severe performance degradation of the SAR imagery.

To mitigate RFIs, many researchers have done lots of works for several decades. These works can be classified into three categories: non-parametric methods, parametric methods, and semi-parametric methods. Non-parametric methods, such as notched filter method [5] and the eigen-subspace projection (ESP) method [6], have been demonstrated to realize really good performance on real SAR systems with good efficiency. But they only employ the power difference between interferences and real echoes without considering their intrinsic properties, hence the interference suppression performance may not be the best. Different from non-parametric methods, parametric methods consider both the amplitude and the phase. An RFI, due to its narrowband property, can be modeled by a sinusoidal signal. Then the RFI suppression problem was transformed to an estimation problem of the sinusoidal model. Several classic methods, such as iterative adaptive approach (IAA) [7] and RELAX algorithm [8], were employed to extract RFIs pulse by pulse. Although the sinusoidal model fits the RFI, the real echoes are not protected when extracting RFIs. Also, it would be computationally expensive for parametric methods since they have to estimate the parameters over multiple iterations and thousands of pulses. In order to improve the performance and protect the real echoes, low-rank recovery techniques with sparse regularization have been widely used for RFI suppression in recent years. These methods are defined as semi-parametric methods since their performance is dependent on the hyperparameters in the optimization problem. The classic robust principal component analysis (RPCA) was first employed to solve this problem [9]. But it uses the convex relaxation, which degrades the final performance. Also, it suffers from high computational burden due to the singular value decomposition (SVD) of large-scale SAR signal matrix. To relieve these problems, the matrix factorization [10] and tensor decomposition [11] were proposed for further improvement on both efficiency and effectiveness. Note that these methods still employ the SVD or the tensor decomposition to update several small matrices in terms of computational burden.

Hence in this paper, an efficient RFI suppression algorithm is proposed via alternating projection scheme with comparable performance and faster convergence compared with the other state-of-the-art (SOTA) semi-parametric methods. Specifically, the low-rank recovery with sparse regularization optimization problem can be solved via two alternating projections. One is to project the signal onto a smooth manifold of rank-r matrices and the other one is to project the signal onto a space of sparse matrices. During the alternating projection, the QR decomposition is used for better efficiency instead of the SVD. We strictly derive the closed-form solutions for each step of the whole optimization problem with fast convergence. The real SAR data, i.e.,

Radarsat-1, with measured RFI is provided to demonstrate the effectiveness of the proposed method.

2 Signal Model

The RFI usually has relatively stable frequency bands and strong power that will share the same frequency bands with wideband SAR systems and surely degrade the imagery quality, even in a long distance. For SAR imaging process, the received signal is usually stacked into the 2-D fast time and slow time domain, that is,

$$y(t,t_s) = x(t,t_s) + r(t,t_s) + n(t,t_s), \tag{1}$$

where t denotes the fast time, t_s denotes the slow time, and $x(t,t_s)$, $r(t,t_s)$ and $n(t,t_s)$ are the real echo, RFI, and noise, respectively. Commonly, the parametric methods modeled the RFIs as the sum of multiple complex sinusoids, which contain K frequency components as

$$\begin{aligned} r(t,t_s) &= \sum_{p=1}^{K} A_i(t,t_s)\exp\left(j2\pi f_p t + j\varphi_p(t,t_s)\right) \\ &= \sum_{p=1}^{K} A'_p(t,t_s)\exp\left(j2\pi f_p t\right), \end{aligned} \tag{2}$$

where $A_p(t,t_s)$, f_p and $\varphi_p(t,t_s)$ denote the amplitude, carrier frequency, and initial phase of the p-th frequency component, respectively. The amplitude and initial phase of each frequency component are rewritten as the complex amplitude $A'_p(t,t_s)$. By stacking all the pulses in (1), the received signal matrix $\mathbf{Y} \in \mathbb{C}^{m\times n}$ is formulated as

$$\mathbf{Y} = \mathbf{X} + \mathbf{R} + \mathbf{N}, \tag{3}$$

where $\mathbf{X}$, $\mathbf{R}$, and $\mathbf{N}$ are the 2-D real echo, RFI, and noise, respectively. In the following subsection, the time-varying RFI model and its characteristics will be analyzed in detail. In previous researches, the RFI matrix $\mathbf{R}$ has been proved to be low rank since its frequency spectrum perform like multiple sinc peaks with stable frequencies, as shown in Fig. 1. Most of the semi-parametric RFI suppression methods constrain the rank of the RFI matrix and add a regularization term of useful signals (i.e., the real echoes), that is, [10]

$$\begin{aligned} \min_{\mathbf{R},\mathbf{X}} \ & \operatorname{rank}(\mathbf{R}) + \lambda \cdot \mathrm{RE}(\mathbf{X}) \\ \text{s.t.} \ & \|\mathbf{Y}-\mathbf{R}-\mathbf{X}\|_F^2 < \delta, \end{aligned} \tag{4}$$

where rank is the rank operation, RE is the regularization function, such as ℓ_1 norm or Frobenius norm, $\|\cdot\|_F$ is the Frobenius norm, and λ and δ are the hyperparameters. The above problem is commonly a non-convex problem, which is NP-hard to solve. Previous researches usually relaxed it to a solvable problem, such as

$$\begin{aligned} \min_{\mathbf{R},\mathbf{X}} \ & \|\mathbf{R}\|_* + \lambda\|\mathbf{X}\|_1 \\ \text{s.t.} \ & \|\mathbf{Y}-\mathbf{R}-\mathbf{X}\|_F^2 < \delta, \end{aligned} \tag{5}$$

where $\|\cdot\|_*$ denotes the nuclear norm, $\|\cdot\|_1$ denotes the ℓ_1 norm. The above problem is a classic robust principal component analysis (RPCA) problem and can be efficiently solved via the alternating direction method of multipliers (ADMM). The nuclear norm is a convex relaxation of the original RFI suppression problem. In [10], it mentioned that the low-rank recovery via the nuclear norm punishes the recovered large singular value too much. The recovered RFI matrix has lower power than the expected one, and then the residual RFI may still interfere with the useful signal. To circumvent this shortcoming, we constrain the RFI matrix with the non-convex rank operation with the convex ℓ_1 norm to regularize the useful signal, then the optimization problem can be written as

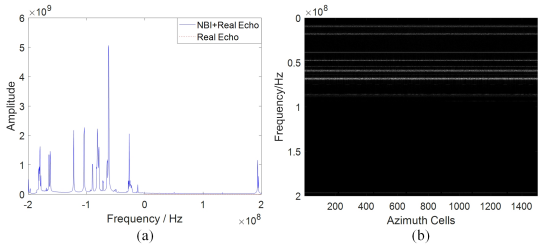

Figure 1. Frequency spectra of measured RFIs. (a) One-snapshot RFI. (b) All-snapshot RFI.

$$\begin{aligned} \min_{\mathbf{R},\mathbf{X}} \ & \|\mathbf{X}\|_1 + \tfrac{\mu}{2}\|\mathbf{Y}-\mathbf{R}-\mathbf{X}\|_F^2 \\ \text{s.t.} \ & \operatorname{rank}(\mathbf{R}) \le r \end{aligned} \tag{6}$$

where r is the estimated rank of RFI matrix. Herein, the above problem can be considered as the combination of the non-convex low-rank recovery and the convex sparse regularization. In the following section, an efficient algorithm would be derived in detail for solving the above problem.

3 Proposed RFI Suppression Algorithm

In this section, we use the alternating projection scheme to solve the optimization problem in (6). The problem can be solved by alternately optimizing the following two subproblems:

$$\begin{aligned} \min_{\mathbf{R}} \ & \|\mathbf{Y}-\mathbf{R}-\mathbf{X}\|_F^2 \\ \text{s.t.} \ & \operatorname{rank}(\mathbf{R}) \le r, \end{aligned} \tag{7}$$

$$\min_{\mathbf{X}} \ \|\mathbf{X}\|_1 + \frac{\mu}{2}\|\mathbf{Y}-\mathbf{R}-\mathbf{X}\|_F^2. \tag{8}$$

It turns out to project $\mathbf{Y}-\mathbf{X}$ onto the space of rank-r matrices and then update $\mathbf{X}$ by projecting $\mathbf{Y}-\mathbf{R}$ onto the space of sparse matrices. To solve the subproblem (7), solutions can be calculated via the singular value decomposition (SVD) followed by truncating out small singular values. However, the SVD operation is computationally expensive, especially for the large-scale HRWS SAR imaging. Some previous researches use matrix factorization technique [10] to perform SVD on two small-scale matrices, which can improve the efficiency. In this paper, we employ the projection scheme to accelerate the algorithm. Suppose at the $(k+1)$-th iteration, we project the $\mathbf{Y}-\mathbf{X}_k$ onto the low-dimensional subspace and then project the intermediate matrix onto the

smooth manifold of the rank-r matrices. At this stage, $\mathbf{R}_k \in \mathbb{C}^{m\times n}$ is a rank-r matrix, so its left and right singular vectors define an $(m+n-r)r$-dimensional subspace

$$\mathbf{T}_k = \left\{ \mathbf{U}_k\mathbf{A}^H + \mathbf{B}\mathbf{V}_k^H \,\middle|\, \mathbf{A}\in\mathbb{C}^{n\times r}, \mathbf{B}\in\mathbb{C}^{m\times r} \right\} \tag{9}$$

where $\mathbf{R}_k = \mathbf{U}_k\Sigma_k\mathbf{V}_k$ is the SVD of $\mathbf{R}_k$. This subspace turns out to be the tangent space of the smooth manifold of rank-r matrices. Given the matrix $\mathbf{Z}_k = \mathbf{Y} - \mathbf{X}_k$, then the projections of $\mathbf{Z}_k$ onto the subspace $\mathbf{T}_k$ is given by

$$\mathscr{P}_{\mathbf{T}_k}\mathbf{Z}_k = \mathbf{U}_k\mathbf{U}_k^H\mathbf{Z}_k + \mathbf{Z}_k\mathbf{V}_k\mathbf{V}_k^H - \mathbf{U}_k\mathbf{U}_k^H\mathbf{Z}_k\mathbf{V}_k\mathbf{V}_k^H \tag{10}$$

To perform the projection onto a smooth manifold of the rank-r matrices, it looks like we need to obtain the new estimate via the SVD of $\mathbf{R}_k$. Inspired by the manifold optimization in [12], it can be computed in an efficient way. Take the QR decompositions of the following matrices

$$\left(\mathbf{I} - \mathbf{U}_k\mathbf{U}_k^H\right)\mathbf{Z}_k\mathbf{V}_k = \mathbf{Q}_1\mathbf{R}_1, \tag{11}$$

$$\left(\mathbf{I} - \mathbf{V}_k\mathbf{V}_k^H\right)\mathbf{Z}_k^H\mathbf{U}_k = \mathbf{Q}_2\mathbf{R}_2, \tag{12}$$

where $\mathbf{I}$ denotes the identity matrix. Then the projection of $\mathbf{Z}_k$ onto the subspace $\mathbf{T}_k$ can be formulated as

$$\begin{aligned}
&\mathscr{P}_{T_k}\mathbf{Z}_k \\
&= \mathbf{U}_k\mathbf{U}_k^H\mathbf{Z}_k\left(\mathbf{I} - \mathbf{V}_k\mathbf{V}_k^H\right) + \left(\mathbf{I} - \mathbf{U}_k\mathbf{U}_k^H\right)\mathbf{Z}_k\mathbf{V}_k\mathbf{V}_k^H + \mathbf{U}_k\mathbf{U}_k^H\mathbf{Z}_k\mathbf{V}_k\mathbf{V}_k^H \\
&= \mathbf{U}_k\mathbf{R}_2^H\mathbf{Q}_2^H + \mathbf{Q}_1\mathbf{R}_1\mathbf{V}_k^H + \mathbf{U}_k\mathbf{U}_k^H\mathbf{Z}_k\mathbf{V}_k\mathbf{V}_k^H \\
&= \begin{bmatrix} \mathbf{U}_k & \mathbf{Q}_1 \end{bmatrix} \begin{bmatrix} \mathbf{U}_k^H\mathbf{Z}_k\mathbf{V}_k & \mathbf{R}_2^H \\ \mathbf{R}_1 & 0 \end{bmatrix} \begin{bmatrix} \mathbf{V}_k^H \\ \mathbf{Q}_2^H \end{bmatrix} \\
&= \begin{bmatrix} \mathbf{U}_k & \mathbf{Q}_1 \end{bmatrix} \mathbf{M}_k \begin{bmatrix} \mathbf{V}_k^H \\ \mathbf{Q}_2^H \end{bmatrix},
\end{aligned} \tag{13}$$

where we have the fact that $\mathbf{U}_k^H\mathbf{Q}_1 = \mathbf{V}_k^H\mathbf{Q}_2 = \mathbf{0}$. Let $\mathbf{M}_k = \mathbf{U}_{M_k}\Sigma_{M_k}\mathbf{V}_{M_k}^H$ be the SVD of $\mathbf{M}_k$. Then we can calculate the SVD of the projection of $\mathbf{Z}$ as

$$\mathbf{U}_{k+1} = \begin{bmatrix} \mathbf{U}_k & \mathbf{Q}_1 \end{bmatrix}\mathbf{U}_{M_k}, \Sigma_{k+1} = \Sigma_{M_k}, \mathbf{V}_{k+1} = \begin{bmatrix} \mathbf{V}_k & \mathbf{Q}_2 \end{bmatrix}\mathbf{V}_{M_k}. \tag{14}$$

After projecting the $\mathbf{Y} - \mathbf{X}_k$ onto the low dimensional subspace, and then we use the truncated SVD to project the intermediate matrix onto the rank-r matrix manifold, that is,

$$\mathbf{R}_{k+1} = \mathscr{H}_r\left(\mathscr{P}_{\mathbf{T}_k}\left(\mathbf{Y} - \mathbf{X}_k\right)\right), \tag{15}$$

where

$$\mathscr{H}_r\left(\mathbf{Z}_k\right) = \mathbf{U}_{k+1}\Sigma_{k+1,r}\mathbf{V}_{k+1}^H, \tag{16}$$

$$\left[\Sigma_{k+1,r}\right]_{ii} = \begin{cases} \left[\Sigma_{k+1}\right]_{ii}, & i \le r \\ 0, & \text{otherwise} \end{cases} \tag{17}$$

Next, we update the useful signal matrix $\mathbf{X}_{k+1}$ via the soft-thresholding algorithm as follows:

$$\mathbf{X}_{k+1} = \mathrm{Sr}\left(\mathbf{Y} - \mathbf{R}_{k+1}, \frac{1}{\mu}\right), \tag{18}$$

where

$$\left[\mathrm{Sr}\left(\mathbf{C}, \beta\right)\right]_{ij} = \max\left\{\left|\mathbf{C}_{ij}\right| - \beta, 0\right\}\frac{\mathbf{C}_{ij}}{\left|\mathbf{C}_{ij}\right|}. \tag{19}$$

The whole algorithm stops when the following termination criterion

$$\frac{\|\mathbf{Y} - \mathbf{R} - \mathbf{X}\|}{\|\mathbf{Y}\|} < \eta \tag{20}$$

holds or the maximum number of iterations is reached.

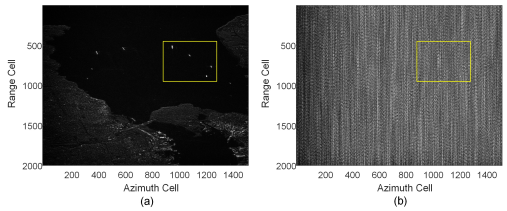

Figure 2. (a) Original RFI-free SAR image. (b) RFI-polluted SAR image.

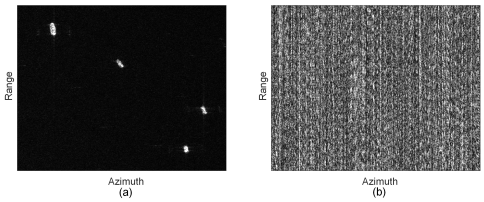

Figure 3. Enlarged regions of the yellow rectangles in Fig. 5. (a) Original RFI-free SAR image. (b) RFI-polluted SAR image.

4 Numerical Experiment

In this section, a numerical experiment of the proposed method for mitigating time-varying RFIs is evaluated on the real SAR data with measured RFIs. Herein, the SAR data and RFIs are separately collected so that we can finely tune the ratios between these two signals to simulate the circumstances of different input signal-to-interference-and-noise ratio (SINR) cases. In order to quantify the performance of the interference suppression methods, the output root-mean-square error (RMSE) is used in the following experiment, which is defined as

$$\mathrm{RMSE}\left(\mathbf{X}, \hat{\mathbf{X}}\right) = \frac{\left\|\mathbf{X} - \hat{\mathbf{X}}\right\|_F}{\|\mathbf{X}\|_F}, \tag{21}$$

where $\mathbf{X}$ is the normalized real echoes and $\hat{\mathbf{X}}$ is the normalized recovered echoes. A smaller RMSE indicates better recovered performance.

For this example, we apply the range-Doppler (RD) imaging algorithm to generate high resolution SAR images. The input SINR is tuned as -20 dB, and as can be seen in Fig. 2, the original RFI-free SAR image and the RFI-polluted SAR image are presented. The whole scene is polluted by strong RFIs and nothing useful can be recognized at all. Also the region in the yellow rectangle is enlarged in Fig. 3. Next, we apply the CLEAN method, RPCA method, the reweighted matrix factorization (RMF) method [10], and the proposed method on the polluted data. The results are shown in Fig. 4 with the enlarged regions shown in Fig. 5. The RMSEs of all methods are listed in the caption. To be fair, all the mentioned algorithms are semi-parametric methods. As can be seen, the CLEAN method, as a typical parametric method, lacks of the real echo protection, so it has the highest RMSE among all the methods. RPCA method uses the convex relaxation with more interference left. The proposed method and the RMF method have bet-

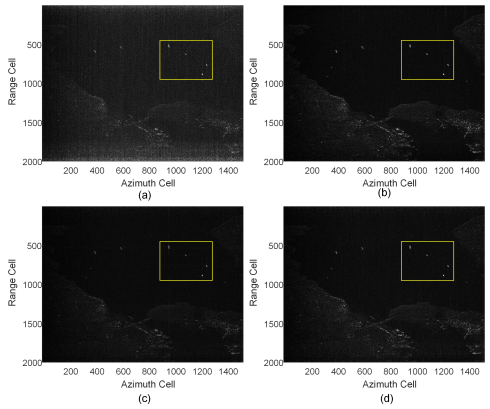

Figure 4. RFI suppression results. (a) CLEAN method. RMSE = 0.8165. (b) RPCA method. RMSE = 0.7990. (c) RMF method. RMSE = 0.5964. (d) Proposed method. RMSE = 0.5719.

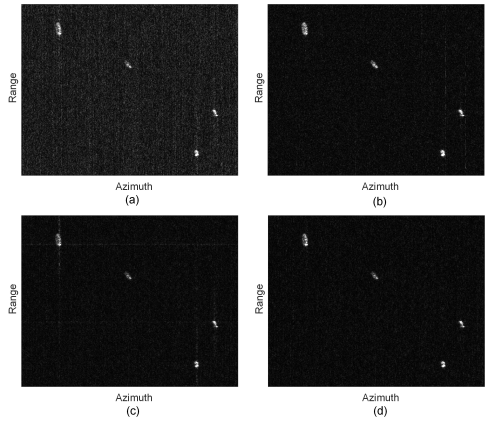

Figure 5. Enlarged RFI suppression results. (a) CLEAN method. (b) RPCA method. (c) RMF method. (d) Proposed method.

ter RFI mitigation performance due to the non-convex low-rank recovery. Moreover, the proposed method has better performance compared with the RMF method. The other main improvement of the proposed method is the computational cost. The CLEAN method, RPCA method, RMF method, and the proposed method take 92.70 s, 28.40 s, 23.87 s, and 7.14 s, respectively, for suppressing RFIs on the desktop with an Intel W-2133 CPU and 256 GB memory. The proposed method greatly improves the efficiency, which would be quite useful for the large-scale SAR imaging.

5 Conclusion

In this paper, we proposed an efficient algorithm for RFI mitigation on SAR systems, which uses the alternating projection scheme and circumvent heavy computational cost resulted from the singular value decomposition (SVD). The real data was used to demonstrate both efficiency and effectiveness of the proposed method compared with the other state-of-the-art semi-parametric methods.

References

[1] Y. Huang, G. Liao, J. Xu, J. Li, D. Yang, "GMTI and Parameter Estimation for MIMO SAR System via a Fast Interferometry RPCA method," *IEEE Trans. Geosci. and Remote Sens.*, **56**, 3, Mar. 2018, pp. 1774-1787.

[2] L. Zhang, M. Xing, C. Qiu, J. Li, J. Sheng, "Resolution enhancement for inversed synthetic aperture radar imaging under low SNR via improved compressive sensing," *IEEE Trans. Geosci. and Remote Sens.*, **48**, 10, 2010, pp. 3824-3838.

[3] Y. Huang, G. Liao, J. Li, J. Xu, "Narrowband RFI Suppression for SAR System via Fast Implementation of Joint Sparsity and Low-rank Property," *IEEE Trans. Geosci. and Remote Sens.*, **56**, 5, May 2018, pp. 2748-2761.

[4] J. D. Taylor, "Introduction to Ultra-Wideband Radar Systems," *Boca Raton, FL: CRC*, 1994.

[5] G. Cazzaniga, A. Guarnieri, "Removing RF interferences from P-band airplane SAR data," *IEEE International Geoscience and Remote Sensing Symposium*, 1996, pp. 1845-1847.

[6] F. Zhou, R. Wu, M. Xing, Z. Bao, "Eigensubspace-based filtering with application in narrow-band interference suppression for SAR," *IEEE Geosci. Remote Sens. Lett.*, **4**, 1, Jan. 2007, pp. 75-79.

[7] Z. Liu, G. Liao, Z. Yang, "Time variant RFI suppression for SAR using iterative adaptive approach," *IEEE Geosci. and Remote Sensing Lett.*, **10**, 6, 2013, pp. 1424-1428.

[8] X. Huang, D. Liang, "Gradual RELAX algorithm for RFI suppression in UWB SAR," *Electronics Letters*, **35**, 22, 1999, pp. 1916-1917.

[9] J. Su, H. Tao, M. Tao, J. Xie, Y. Wang, L. Wang, "Time-Varying SAR Interference Suppression Based on Delay-Doppler Iterative Decomposition Algorithm," *Remote Sensing*, **10**, 9, 2018, pp. 1491-1509.

[10] Y. Huang, G. Liao, Z. Zhang, Y. Xiang, J. Li, A. Nehorai, "Fast Narrowband RFI Suppression Algorithms for SAR Systems via Matrix-Factorizatoin Techniques," *IEEE Trans. Geosci. and Remote Sens.*, **57**, 1, 2019, pp. 250-262.

[11] Y. Huang, L. Zhang, J. Li, Z. Chen, X. Yang, "Reweighted Tensor Factorization Method for SAR Narrowband and Wideband Interference Mitigation Using Smoothing Multiview Tensor Model," *IEEE Trans. Geosci. and Remote Sens.*, **58**, 5, 2020, pp. 3298-3313.

[12] B. Vandereycken, "Low-Rank Matrix Completion by Riemannian Optimization," *SIAM Journal on Optimization*, **23**, 2, 2013, pp. 1214-1236.